Effect of Strain on the Properties of an Ethylene–Octene Elastomer with Conductive Carbon Fillers

L. FLANDIN, A. CHANG, S. NAZARENKO, A. HILTNER, E. BAER

Department of Macromolecular Science and Center for Applied Polymer Research, Case Western Reserve University, Cleveland, Ohio 44106-7202

Received 13 July 1999; accepted 16 September 1999

ABSTRACT: Composites that incorporate a conductive filler into an ethylene–octene (EO) elastomer matrix were evaluated for DC electrical and mechanical properties. Comparing three types of fillers (carbon fiber, low structure carbon black, and high structure carbon black), it was found that the composite with high structure carbon black exhibited a combination of properties not generally achievable with this type of filler in an elastomeric matrix. A decrease in resistivity at low strains is unusual and has only been reported previously in a few instances. Reversibility in the resistivity upon cyclic deformation is a particularly unusual feature of EO with high structure carbon black. The mechanical and electrical performance of the high structure carbon black composites at high strains was also impressive. Mechanical reinforcement in accordance with the Guth model attested to good particle–matrix adhesion. The EO matrix also produced composites that retained the inherent high elongation of the unfilled elastomer even with the maximum amount of filler (30% by volume). The EO matrix with other conducting fillers did not exhibit the exceptional properties of EO with high structure carbon black. Composites with carbon fiber and low structure carbon black did not maintain good mechanical properties, generally exhibited an increase in resistivity with strain, and exhibited irreversible changes in both mechanical and electrical properties after extension to even low strains. An explanation of the unusual properties of EO with high structure carbon black required unique features of both filler and the matrix. The proposed model incorporates the multifunctional physical crosslinks of the EO matrix and dynamic filler–matrix bonds. © 2000 John Wiley & Sons, Inc. J Appl Polym Sci 76: 894–905, 2000

Key words: ethylene–octene copolymer; carbon black; carbon fiber; composites; mechanical properties; electrical properties

INTRODUCTION

Low resistivity elastomers typically employ vulcanized rubber as a matrix for dispersion of a large variety of fillers, mainly carbon blacks,[1,2] carbon fibers,[3] and metallic particles.[4] In addition to imparting conductivity, the filler generally improves environmental resistance and mechanical properties. Because these composites do not always exhibit the best balance of properties, alternative elastomeric matrices are of interest.

In recent years, the development of Dow's INSITE constrained geometry catalyst technology has led to the production of a new class of elastomers based on homogeneous ethylene–α-olefin copolymers. In particular, copolymers with more than 8 mol % octene possess low crystallinity and

Correspondence to: A. Hiltner.

Contract grant sponsor: Army Research Office; contract grant number: DAAG55-98-1-0311.

Contract grant sponsor: National Science Foundation; contract grant number: INT-9726537.

Journal of Applied Polymer Science, Vol. 76, 894–905 (2000)

© 2000 John Wiley & Sons, Inc.

Table I Carbon Black Characteristics

	Particle Diameter (nm)	Structure (DBPA Number)	Surface Area (m^2/g)	Volatiles (%)
Conductex 975U	21	170	242	1
Printex 30	27	102	80	1
MS-TS	300	33	8	1

rubber-like behavior that depends on physical rather than chemical junctions.[5] The main advantage of these polymers over chemically vulcanized elastomers lies in their ease of processing and postprocessing, much like conventional polyethylenes. These elastomeric materials have been commercialized and are the subject of numerous investigations as unfilled polymers[6–8]; however, very little is known about their mechanical and electrical properties when reinforced with conducting fillers.[9]

Electrical properties of binary mixtures depend strongly on the microstructure. In particular, dispersion state,[10] filler geometry,[11] and filler–filler,[10] and filler–matrix[12] interactions strongly affect the electrical properties of composite materials. External variables such as temperature[13,14] and mechanical stretching[15,16] can significantly affect the microstructure and thereby the macroscopic conductivity. If there is a simple relationship between electrical conductivity and an external variable, the composite has potential applications as a sensor.[16]

In the present study, three types of conducting fillers (carbon fiber, high structure carbon black, and low structure carbon black) were incorporated in an ethylene–octene elastomer. The mechanical behavior was studied as a function of filler content in order to quantify the reinforcement effect of the particles. However, the work focused primarily on *in situ* changes of resistivity during uniaxial stretching. The electrical and mechanical properties were analyzed for the purpose of correlating macroscopic behavior with microstructural events.

MATERIALS AND METHODS

Materials

An ethylene–octene (EO) elastomer with density 0.863 g/cc (DEG-8180 from Dupont Dow Elastomers) was the matrix in this study. The fillers were a carbon fiber (CF) (DKDX from Amoco Chemical Co. with diameter 10 μm and aspect ratio 20), a low structure carbon black (LSCB) (MT-ST from Columbian Chemical Co.), and two high structure carbon blacks (HSCB) (Printex 30 from Degussa Corp. and Conductex 975 Ultra from Columbian Chemical Co.). The characteristics of the carbon blacks as provided by the manufacturer are given in Table I.

Blending was carried out in a Haake Rheomix 600 mixing head operating at 40 rpm and 200°C. The polymer was mixed without filler for 1 min until melted and the filler was added slowly over a period of 10 min. Attempts to prepare compositions higher than 30% (v/v) Printex 30 and 25% (v/v) 975U were not successful because the amount of elastomer was insufficient to completely wet and disperse the filler. All the blends as well as the unfilled elastomer were processed under identical conditions. Compression molded plaques were prepared by sandwiching the polymer between Mylar sheets, heating at 200°C for 2 min under minimal pressure followed by repeated pressure cycling between 0 and 700 psi to remove air bubbles. Plaques were rapidly cooled to ambient temperature. To determine the quality of dispersion, specimens were cryofractured in liquid nitrogen, coated with 10 nm of gold and examined in the JEOL JSM-840A scanning electron microscope.

Methods

Stress–strain behavior in uniaxial tension was measured at ambient temperature with microtensile specimens (ASTM 1708) cut from the compression molded plaques. The separation of the grips was 22.3 mm and included the fillet section. The specimen width was 4.8 mm. Specimens were deformed in an Instron 1123 testing machine at a rate of 0.2%/min. Marks were drawn on the spec-

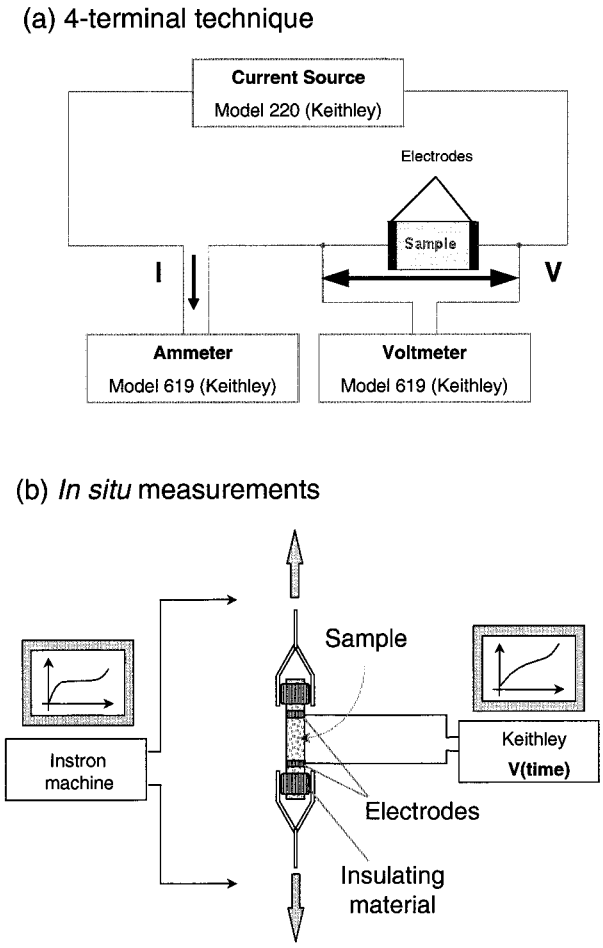

Figure 1 Schematics of DC electrical measurements (a) the 4-terminal technique, and (b) *in situ* during uniaxial extension.

imens and a video recording of the test was made in order to measure the draw ratio.

Electrical properties were measured with a four-terminal technique using a Keithley model 220 as current source and a Keithley model 619 for voltage and current measurements [Fig. 1(a)]. The device was interfaced to a computer to record and process data. The minimum time required to obtain a measurement was 0.1 s. The error in the measurements, determined with standard resistances, was less than 2% for current in the range 10^{-7} to 10^{-2} A and voltage in the range 10^{-5} to 10^{2} V.

To measure changes in conductivity during stretching, strips with initial length L_0 = 135 mm, width W_0 = 10 mm, and thickness H_0 = 2 mm were cut from the plaques. For electrical measurements along the length (parallel direction) flat clamps covered with copper foil were used. The clamps applied an approximately constant pressure even on strained specimens and could therefore be used to measure resistance during deformation to fracture [Fig. 1(b)]. For electrical measurements through the thickness (perpendicular direction), electrodes were made by depositing a thick layer of gold (≈200 nm) on the surfaces. The specimen was mounted in the Instron and the stress σ, specimen length L, and voltage were recorded during extension. The applied current was 10^{-5} A unless at higher strains the voltage approached the limit of the device, in which case the current was decreased. When this occurred, the resistance changed very slightly, indicating that deformation did not alter the ohmic behavior of the materials.

The resistivity ρ was obtained from the measured resistance and the geometrical changes in the specimen. The constant volume assumption, i.e., a Poisson's ratio of 0.5, is generally considered valid for polymers above the glass transition temperature. With this assumption, the resistivity parallel and perpendicular to the extension direction were given respectively by

$$\rho_{\parallel} = R_{\parallel} \frac{WH}{L} = R_{\parallel} \frac{V_0}{L^2} \tag{1}$$

$$\rho_{\perp} = R_{\perp} \frac{WL}{H} = R_{\perp} \frac{W_0 L}{H_0} \tag{2}$$

By using eqs. (1) and (2) to calculate resistivity, the volume V_0 was assumed constant and possible volume changes due to void formation were neglected.

RESULTS AND DISCUSSION

Electrical Properties Without Strain

Scanning electron micrographs of the cryofractured composites indicated that the fillers were well dispersed in the ethylene–octene (EO) matrix. In Figure 2(a), bare surfaces of pulled-out carbon fibers (CF) and corresponding holes in the matrix left by pulled-out fibers indicated that adhesion between matrix and fibers was poor. The particles of the low structure carbon black (LSCB) appeared to be embedded in the fracture surface [Fig. 2(b)], suggesting good adhesion between particles and matrix in this composite. The fracture surface of the high structure carbon black (HSCB)

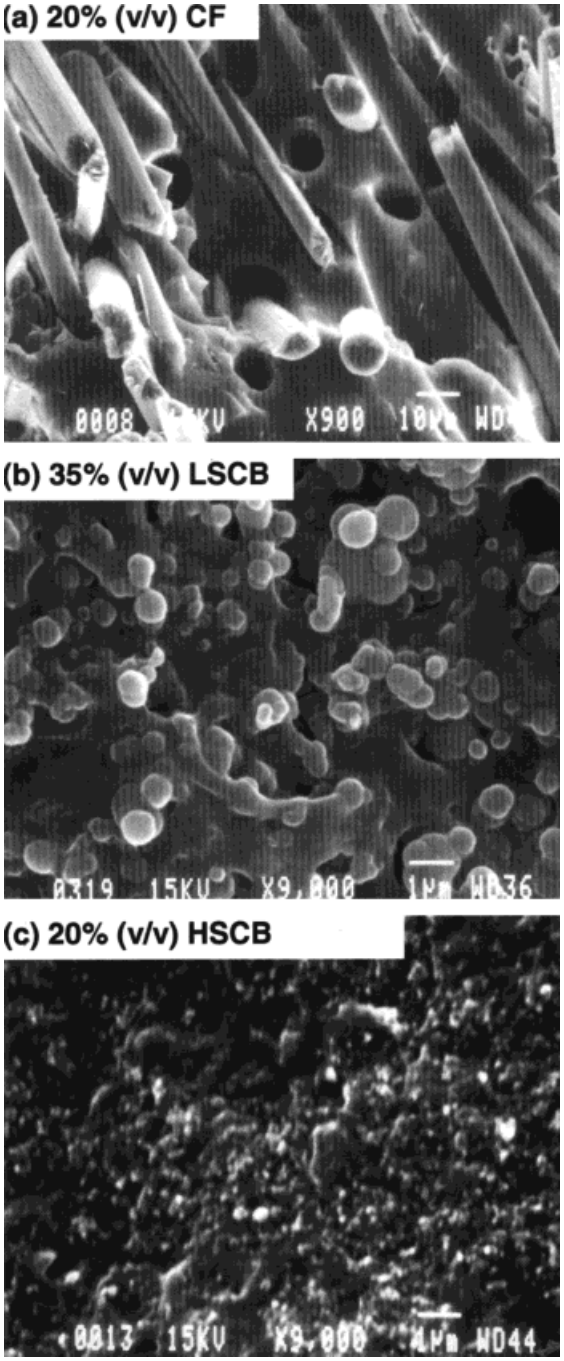

Figure 2 Scanning electron micrographs of cryofracture surfaces: (a) EO with 20% (v/v) carbon fibers, (b) EO with 35% (v/v) low structure carbon black, and (c) EO with 20% (v/v) high structure carbon black (Printex).

composite revealed a uniform dispersion of very small particles [Fig. 2(c)]. The particle size of 50–300 nm indicated that these were the primary aggregates.

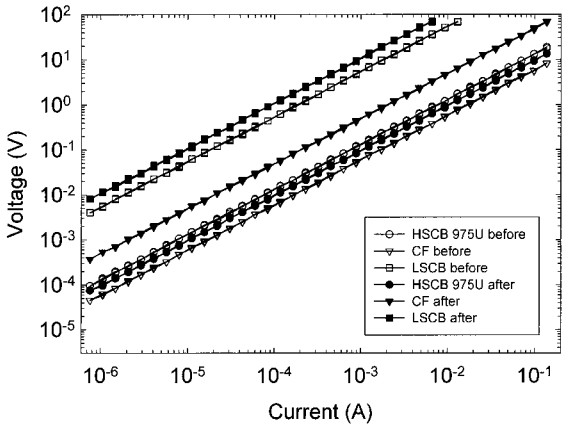

Figure 3 Current–voltage relationship of EO with 20% (v/v) CF, 45% (v/v) LSCB, and 20% (v/v) HSCB (975U) before (open symbols) and after (solid symbols) straining to 20%.

All the composites exhibited ohmic behavior over the current range used to measure the electrical properties (Fig. 3). Linear behavior indicated that the conducting pathway existed in the as-processed materials and was not altered by application of voltage. Stretching did not compromise the ohmic behavior. The response remained linear after the materials were stretched to 20% strain and allowed to recover for 1–2 h.

The resistivity as a function of filler content showed the typical S-shaped dependency with three regions (dielectric, transition and conductive) (Fig. 4). Specimens with low filler content were almost nonconductive. However, at a critical composition that depended on the specific filler, the resistivity fell sharply into the range of 1–10

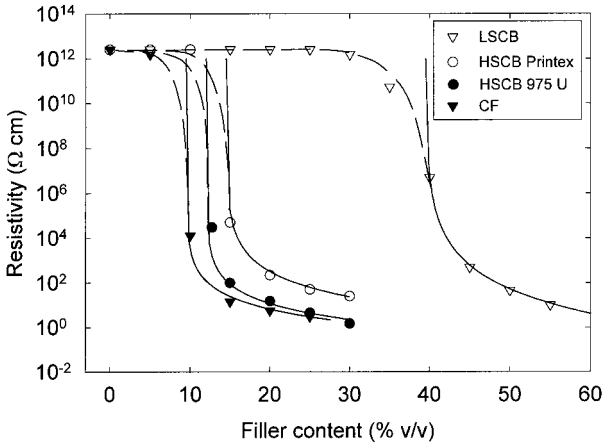

Figure 4 Resistivity as a function of filler content. The solid lines are the statistical percolation fit.

Table II Percolation Parameters for EO Composites

Filler	t	V_c (vol%)
HSCB (975U)	2.05	12
HSCB (Printex 30)	2.55	14.5
LSCB (MT-ST)	3.80	39.5
CF (DKDX)	2.04	9.5

ohm cm. Assuming that the critical filler content corresponded to a percolation threshold, the HSCB and CF composites formed a continuous network with 10–15% (v/v) filler, which was considerably less than the 40% (v/v) required for the LSCB composite. A value of 20–40% (v/v) is typical of spherical particles. The high aspect ratio of the fibers, and the aggregate form of the high structure carbon black, which increased the probability of particle–particle contacts, accounted for the low percolation thresholds.[2]

The resistivity of a dispersion of conductive particles in an insulating matrix at and above the percolation threshold is generally modeled by a power law relationship[17–19]

$$\frac{1}{\rho} = \left(\frac{V - V_c}{1 - V_c}\right)^t \tag{3}$$

where V is the volume fraction of filler, V_c is the percolation threshold, and t is the exponent that characterizes the "strength" of the transition. The exponent t is assumed to depend only on the dimensionality of the system, and for a three-dimensional system is about 2.[20] The fits of eq. (3) are included in Figure 4 as the solid lines and the corresponding parameters are given in Table II. The data fit well with t close to 2 except for the LSCB composites. This filler differed from the others with a t value of about 4 and a significantly higher value of V_c. Although values of t larger than 2 have often been measured,[21] the reason for the high value of LSCB-filled EO is not clear.

Mechanical Properties

Engineering stress–strain curves of the CF composites are shown in Figure 5. The initial modulus increased significantly with the addition of fibers. Specimens with filler content below the percolation threshold deformed uniformly until they fractured at a stress and strain that were comparable to the fracture characteristics of the unfilled polymer. At and above the percolation threshold, yielding with formation of a well-defined neck was observed. The magnitude of the accompanying stress drop increased with the filler content; furthermore, the fracture strain decreased precipitously. The tendency for fiber-filled elastomers to yield, sometimes below the percolation threshold, has been observed previously.[22,23] The formation of an instability was related to debonding of the fibers from the matrix and subsequent formation of cavities that acted as flaws. The local stress concentration increased the local strain and a necking instability resulted.

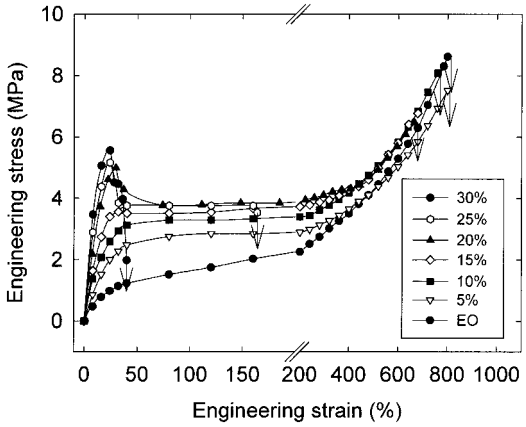

Figure 5 Stress–strain curves of composites with various amounts of CF.

Stress–strain curves of LSCB composites, plotted as engineering stress vs draw ratio in Figure 6, show the reinforcing effect of the filler on the initial modulus. Compositions below the percolation threshold extended to high strains comparable to the fracture strain of the unfilled elastomer.

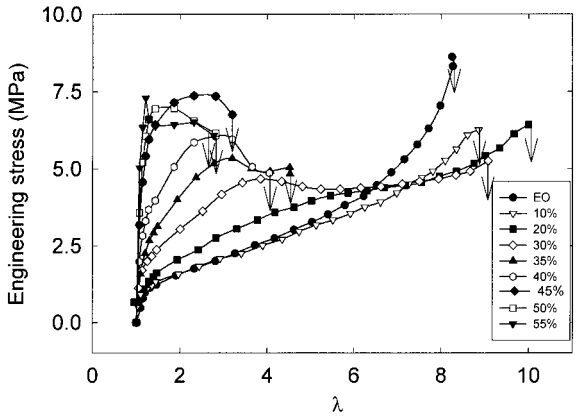

Figure 6 Stress–strain curves of composites with various amounts of LSCB.

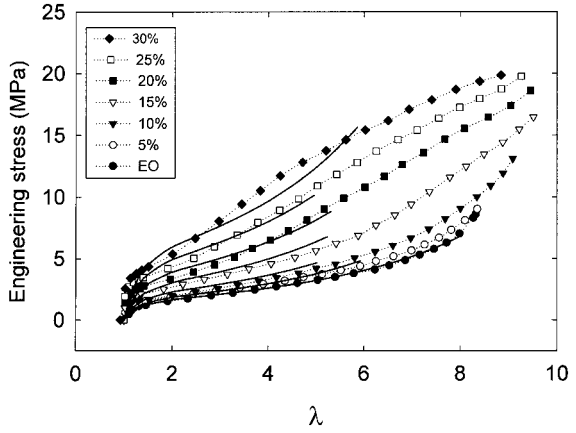

Figure 7 Stress–strain curves of composites with various amounts of HSCB (Printex). The solid lines are the fit to the Guth model, with $f = 3.53$.

As the composition approached and exceeded the percolation threshold, the fracture strain decreased dramatically. In contrast to the CF-filled elastomer, all the compositions deformed uniformly without necking; however, the shape of the stress–strain curve gradually changed with the appearance of a broad maximum at intermediate strains. An indication of the maximum appeared in the stress–strain curve of the 20% (v/v) composition, and a distinct maximum became visible with higher filler contents. The maximum gradually shifted to higher stresses and lower strains as the filler content increased. This stress softening was not due to formation of a neck, but was attributed to debonding of the particles followed by relaxation of the polymer matrix.

Stress–strain curves of composites with HSCB (Printex) are shown in Figure 7. Similar behavior was observed with another HSCB (975U). All the compositions deformed uniformly to a strain equal to or slightly higher than that of the unfilled elastomer. As the filler content increased to 30% (v/v), gradual increases in the initial modulus, the stress level at intermediate strains, and the tensile strength were observed. Especially at low and intermediate strains, the stress–strain curves took the same shape as the unfilled elastomer, although they shifted to higher modulus values as the filler content increased. The changes appeared to be smooth with no transitional behavior in the vicinity of the percolation threshold.

The effects of the various types of filler on the fracture strain are compared in Figure 8. Compositions with CF or LSCB exhibited a distinct decrease in the fracture strain in the vicinity of the percolation threshold. When these fillers debonded from the matrix, the percolating network offered a weak pathway for the crack to follow through the specimen. The compositions with HSCB (Printex and 975U) were unusual in that they did not exhibit a dramatic decrease in fracture strain at the percolation threshold. This characteristic of EO composites is in contrast to vulcanized elastomer composites, which typically exhibit a decrease in elongation if filled with moderate amounts of high structure carbon black.[24,25]

The most widely used models for the change in modulus of a filled elastomer are the Guth hydrodynamic models.[26] The model for spherical reinforcing particles with perfect adhesion has the form

$$G = G_0(1 + 2.5V + 14.1V^2) \tag{4}$$

where G is the modulus of the filled elastomer, G_0 is the modulus of the unfilled elastomer, and V is the volume fraction filler. According to this formula, the particles shift the entire stress–strain curve by a factor that depends only on the amount of filler. Moreover, superposition is not bound to the specific theoretical stress–strain relation of the matrix. Only HSCB appeared to produce this characteristic. To test the possibility that the curves would superpose with a simple shift factor, the data for one HSCB (Printex) are plotted in Figure 9 as the rubber modulus $G = \sigma(\lambda - 1/\lambda^2)^{-1}$, where λ is the extension ratio and σ is the engineering stress. The curves for the composites were shifted by a factor α to obtain the best overlap with the unfilled matrix. A gradually

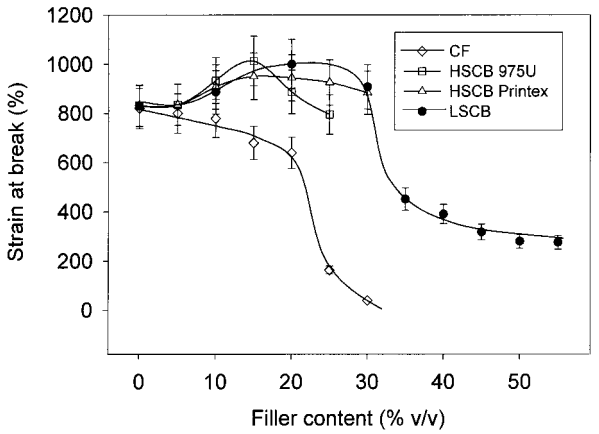

Figure 8 Effect of filler content on the fracture strain of EO composites.

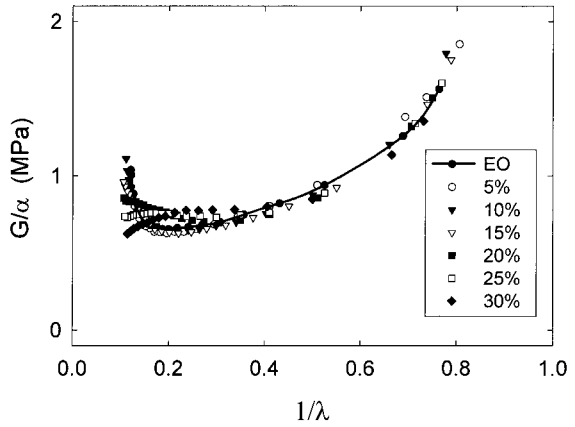

Figure 9 Rubber modulus $G = \sigma(\lambda - 1/\lambda^2)^{-1}$ of composites with various amounts of HSCB (Printex) shifted to the modulus G_0 of unfilled EO by a shift factor α.

decreasing modulus at low strains was followed by a region of almost constant modulus. Especially at low and intermediate strains, the stress–strain behavior superposed well. Deviations toward lower modulus values at higher strains, especially with the higher filler contents, were consistent with loss of particle–matrix adhesion.

The shift factors used to obtain superposition are plotted in Figure 10. The values were different for the two high structure carbon blacks, and were higher than predicted by eq. (4). If the particles are nonspherical, eq. (4) is replaced by the expression

$$G = G_0(1 + 0.67fV + 1.62f^2V^2) \qquad (5)$$

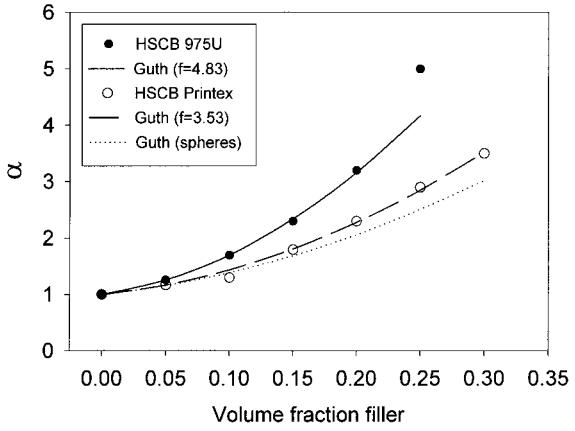

Figure 10 Comparison of the shift factors for HSCB composites with the Guth models for spherical particles [dotted line, eq. (4)], and rodlike particles [dashed and solid lines, eq. (5)].

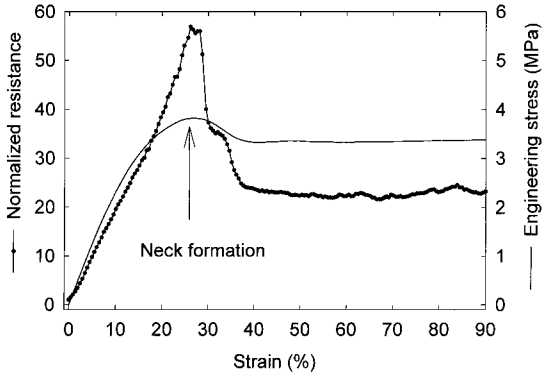

Figure 11 Change in normalized resistance during deformation of a composite with 20% (v/v) CF.

where f is the particle aspect ratio (length/width). With f as an adjustable parameter, excellent fits were obtained with $f = 3.53$ for Printex and $f = 4.83$ for 975U. The only exception was the composite with 25% (v/v) 975U. Stress–strain curves of Printex composites calculated from the shift factors obtained from eq. (5) with $f = 3.53$ and the stress–strain relationship of unfilled EO are included in Figure 7 as the solid lines. Good correlation between the model and experiment extended to relatively high strains, approximately $\lambda = 5$. The magnitude of f for 975U was comparable to the average aspect ratio provided by the manufacturer of 2.78. However, it should be noted that eq. (5) applies for rigid rods of relatively high aspect ratio, and although the high structure carbon black particles possess an irregular shape, the parameter f should not be literally interpreted as the aspect ratio of the particles.

Electrical Properties Under Uniaxial Strain

The change in electrical properties that accompanied deformation of the elastomer with 20% (v/v) CF is shown in Figure 11 as the resistance normalized to the resistance of the unstressed specimen. The resistance increased rapidly as the strain increased to the yield point at about 30% strain. The factor by which the resistance increased varied between 40 and 80 from one specimen to another. Nevertheless, the relative increase in resistance with this filler was much higher than was observed in other carbon fiber-filled elastomers.[23] If the neck formed between the electrodes, the resistance sharply increased further to a value outside the measurable range of the apparatus. The high local strain in the neck effectively destroyed the conductive network and

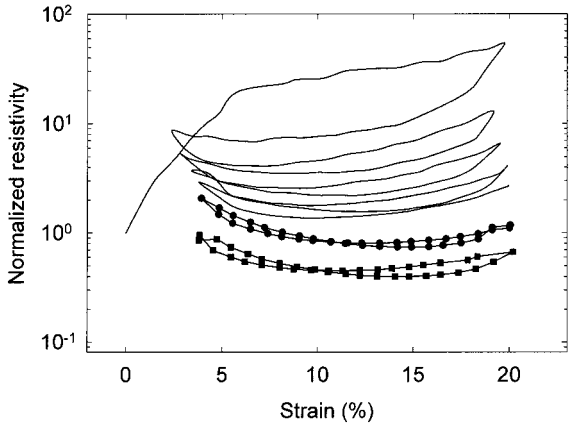

Figure 12 Effect of cyclic deformation to 20% strain on the normalized resistivity of a composite with 20% (v/v) CF. Cycles 1–5 (solid lines), cycle 10 (circles), and cycle 30 (squares). $\rho_{0\|}$ = 6.3 Ωcm.

the result was largely irreversible. The permanently deformed necked material remained a good insulator even after the stress was removed and the specimen was allowed to recover for a period of time. If the neck formed outside the electrodes, as in the example in Figure 11, the resistance dropped in two steps to a value that remained constant as the neck propagated. The first drop was due to retraction of the unnecked material as the neck formed and the engineering stress decreased, the second drop to the final value was attributed to viscoelastic relaxation of the matrix.

Repeated cycling to 20% strain produced the normalized resistivity curves of the 20% CF composite in Figure 12. The normalized resistivity decreased precipitously after the first loading. It gradually decreased further, as shown by the succeeding loading and unloading cycles (2nd–5th cycles and 10th cycle); and continued to decrease up to the 30th cycle when the experiment was terminated. Presumably this was due to formation of additional conducting pathways by breakdown of matrix material between carbon fibers.

The resistance of the composite with 45% (v/v) LSCB initially increased rapidly, and continued to increase monotonically during uniform deformation until it reached the limit of the apparatus (Fig. 13). The normalized parallel and perpendicular resistivities are plotted on a linear scale to emphasize the difference between them in the low strain region. The continuously increasing parallel resistivity included a small plateau region of lower slope in the region of 5–10% strain. In the

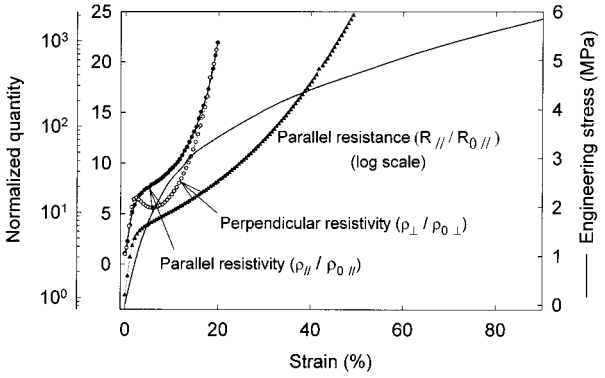

Figure 13 Change in normalized electrical properties during deformation of a composite with 45% (v/v) LSCB.

same strain region, the perpendicular resistivity exhibited a maximum followed by a minimum. At higher strains, the parallel and perpendicular resistivities essentially superposed.

Initially the resistivity of the 45% (v/v) LSCB composite was about an order of magnitude larger in the perpendicular direction than in the parallel direction; this anisotropy probably resulted from the compression molding procedure, which required repeated application and release of pressure to remove air bubbles. Therefore the electrical response during cycling is presented as the normalized resistivity in Figure 14. The behavior qualitatively resembled that of the CF composite. A pronounced minimum on the first unloading curve resulted from a decrease in resistivity followed by an increase as the strain was reduced to the set strain of 5%. Subsequent loading and un-

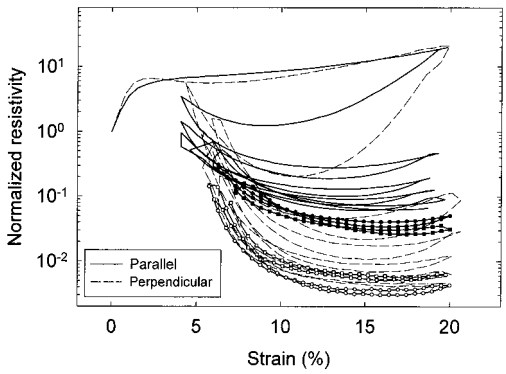

Figure 14 Effect of cyclic deformation to 20% strain on the normalized resistivity of a composite with 45% (v/v) LSCB. Cycles 1–5 (solid and dashed lines), cycle 10 (circles), and cycle 30 (squares). $\rho_{0\|}$ = 500 Ωcm, $\rho_{0\perp}$ = 4800 Ωcm.

loading cycles were characterized by an initial decrease in resistivity on loading and a corresponding increase on unloading. The overall resistivity gradually decreased with continued cycling to the 30th cycle. The parallel and perpendicular curves had the same shapes; however, the decrease in normalized resistivity on the first cycle was much larger in the perpendicular direction than in the parallel direction, and the perpendicular resistivity always decreased considerably more on the loading curve than the parallel resistivity. This was probably a Poisson's effect. Extension reduced the thickness and increased the number of particle contacts by bringing particles closer together. This decreased the resistivity in both directions, but more so in the perpendicular direction. To a large extent, the strain-induced contacts were lost when stress was removed; however, as cycling proceeded, permanent changes occurred and there was a gradual decrease in the resistivity.

The effect of strain on the resistance of the composite with 20% (v/v) HSCB (Printex) differed significantly from the behavior of either CF or LSCB composites. After a slight increase in resistance to about 1.5 times the initial value at 2–4% strain, the resistance decreased to a broad minimum at approximately 20% strain where the resistance was about half the initial value (Fig. 15). With further increase in strain, the resistance gradually increased until it eventually exceeded the limit of the apparatus; this occurred close to the fracture strain for this composition. The trend was the same for both parallel and perpendicular resistivities, although the relative decrease in resistivity was larger in the perpendicular direction than in the parallel direction.

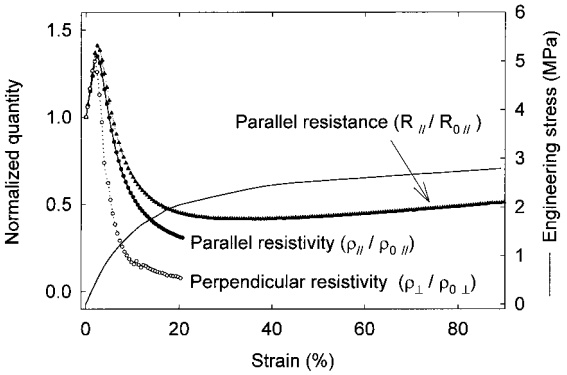

Figure 15 Change in normalized electrical properties during deformation of a composite with 20% (v/v) HSCB (Printex).

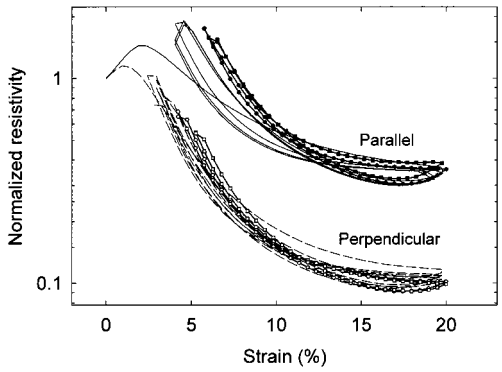

Figure 16 Effect of cyclic deformation to 20% strain on the normalized resistivity of a composite with 20% (v/v) HSCB (Printex). Cycles 1–5 (solid and dashed lines), cycle 10 (circles), and cycle 30 (squares). $\rho_{0\|}$ = 220 Ωcm, $\rho_{0\perp}$ = 750 Ωcm.

The shape of the loading-unloading resistivity curves of the 20% (v/v) HSCB composite somewhat resembled those of the LSCB composite with a decrease in normalized resistivity on loading and a corresponding increase on unloading (Fig. 16). However, there was a fundamental difference in HSCB composites. The response on the first loading was closely reproduced on subsequent cycles. As a result the responses on the 1st through the 30th loading–unloading cycles virtually superposed.

Microstructural Models

The EO elastomer filled with high structure carbon black exhibited a combination of properties not generally achievable with this type of filler in an elastomeric matrix. A decrease in resistivity at low strains is unusual and has only been reported in a few instances. The phenomenon was described recently with a similar composite of carbon black in an EO matrix.[27] The novelty was recognized, but the phenomenon was not studied in depth. A similar phenomenon was reported in silicone rubber filled with a flexible Ni fiber.[28] However, most elastomeric matrices with high structure carbon black, including silicone rubber,[16] exhibit the opposite behavior at low strains with an increase in resistivity upon stretching. In cases where a decrease in resistivity is observed in vulcanized rubber composites, it generally occurs at strains an order of magnitude higher.[29]

Reversibility in the resistivity upon cyclic deformation is a particularly unusual feature of EO with high structure carbon black. In comparison,

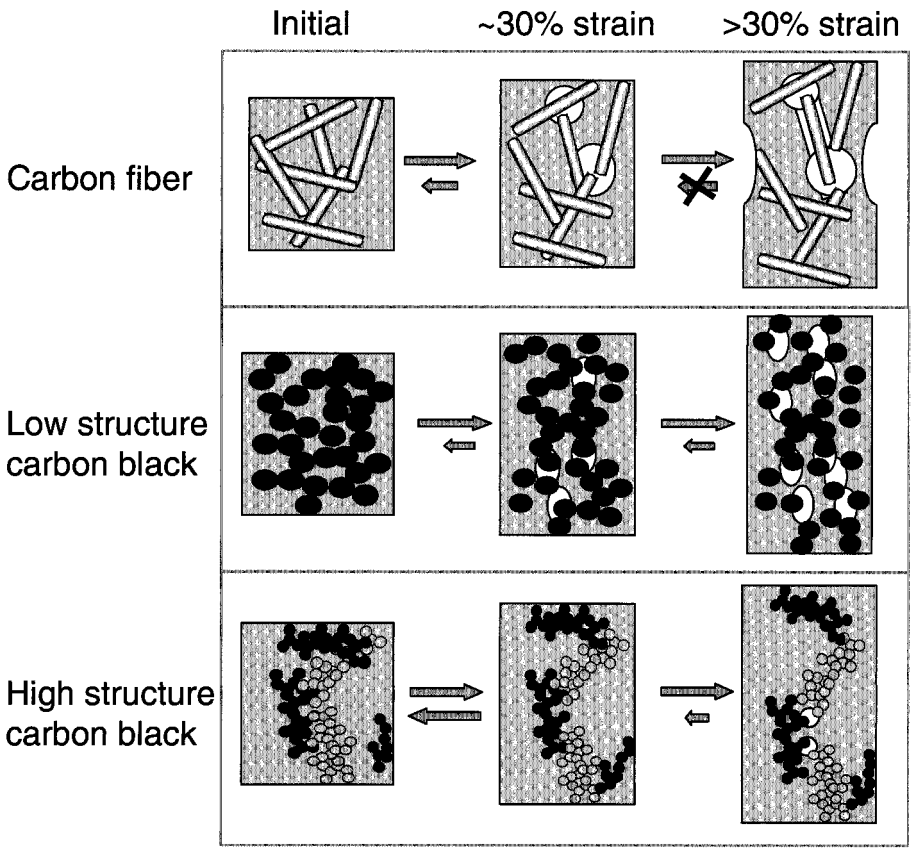

Figure 17 Microstructural models of deformation.

cyclic deformation of silicone rubber with Ni fiber produced a progressive increase in resistivity. Reversibility has been achieved with high structure carbon black in silicone rubber, but only after mechanical preconditioning.[30] In this instance, as in most cases, the resistivity increased upon stretching. The EO matrix differs from many elastomers that have been filled with high structure carbon black by producing a composite that retains the inherent high elongation of the unfilled elastomer even with the maximum filler content of 30% (v/v). Typically, a decrease in elongation at break is observed even with high structure carbon blacks.

It is also instructive that the EO elastomer with other conductive fillers did not exhibit the exceptional properties of EO with high structure carbon black. Composites with carbon fiber and low structure carbon black did not maintain good mechanical properties, generally exhibited an increase in resistivity with strain, and exhibited irreversible changes in both mechanical and electrical properties after extension to even low strains. An explanation of the unusual properties of EO with high structure carbon black would appear to require unique features of both filler and matrix.

The change in resistivity upon straining a conductive elastomer is generally explained in terms of two simultaneous processes that operate on a continuous conductive network of particles in an insulating matrix. Rotation and translation of asymmetric particles preserves the number of contacts and hence the number of conducting pathways in the direction of stretching. In opposition to this effect, elongation also causes breakage of the existing continuous conducting network by increasing the gap between particles. In general, the effects are perceived as off-setting if the dependence of resistivity on strain is weak, or as dominated by network destruction if the resistivity increases with strain.[23,30] The latter situation appears to apply to EO composites with carbon fiber and low structure carbon black. The increase in resistivity at low strains suggests that the network is broken by loss of contacts as illustrated schematically in Figure 17. The structural changes, and corresponding electrical properties,

are not completely reversible upon unloading. At higher strains additional hole formation leads to necking of the carbon fiber composite and loss of ductility of the low structure carbon black composites.

For high structure carbon blacks, rotation and translation, or possibly shape changes of the asymmetric aggregates, can reduce resistivity. However, particle movement can be inhibited by the permanent network structure of the conventional vulcanized elastomer.[13,14] In contrast to a vulcanized elastomer, the concept of a network of flexible chains with fringed micellar crystals serving as the multifunctional junctions provides the structural basis for EO elastomers. A single polymer molecule contains many segments that are long enough to crystallize; these can be incorporated into different crystals to form a network. The fringed micellar junctions are not fixed, but are thought to provide a sliding topological constraint by a process of detachment–attachment that can also be viewed as partial melting.

It can be imagined that the very small particles of high structure carbon black are less constrained during elongation if they are incorporated into a network of mobile junctions than if the network has fixed junctions. Rather than causing hole formation and destruction of the conducting network, deformation produces new conducting pathways or improvement of existing pathways by particle reorientation (Fig. 17). The effect should be particularly noticeable in the transverse direction, which undergoes contraction during straining due to Poisson's effect. With hole formation prevented, the structural changes, and corresponding electrical properties are essentially reversible upon unloading.

The performance of the high structure carbon black composites at high strains was also impressive. Mechanical reinforcement in accordance with the Guth model attested to good particle–matrix adhesion. Although good particle adhesion typically has a deleterious effect on ultimate elongation of composites with more conventional fillers, good ductility and low resistivity suggested that composites of EO with high structure carbon black tolerated high strains with very little damage accumulation. A mode of adhesion is suggested by analogy to the bound rubber models proposed for vulcanized elastomers. Linear chain segments that are not part of a fringed micellar crystal are ideal candidates for adsorption to the step-like edges of the carbon black particle. Additionally, it is suggested that the particle–matrix bond is dynamic. Although particle–matrix adhesion probably is not disrupted by the relatively low strains where mechanical and electrical properties are reversible, the stresses at higher strains may overcome the physical bond. The shortest or most strained chain segments are affected first and reorganize to increase the connecting length between particles. This constitutes a type of "self-healing" mechanism that reduces damage processes such as debonding and fragmentation of primary aggregates that would lead to hole formation in the conducting network (Fig. 17). The contribution from this type of mechanism should strongly depend on the size scale of the filler particles and on the specific surface structure. For fillers with less interface and fewer sites for particle–matrix bonds, like carbon fiber and low structure carbon black, interfacial damage should heal less easily and more interfacial failure should be experienced. Additional studies probe the electrical and mechanical response of composites with high structure carbon black further.[31] Analysis of reversible and irreversible phenomena, particularly under high strains that can cause damage to the percolating network, is undertaken for the purpose of correlating macroscopic response with microstructural events.

CONCLUSIONS

An ethylene–octene elastomer was evaluated as an alternative matrix to vulcanized rubbers for low resistivity elastomers. Significant differences in electrical and mechanical properties were found among the three conducting fillers used in the study (carbon fiber, low structure carbon black, and high structure carbon black):

1. In terms of percolation behavior, composites with low structure carbon black had a higher percolation threshold (~40% v/v compared to ~10% v/v) and a "softer" transition as indicated by a higher exponent in the power law relationship for resistivity.
2. All the fillers provided mechanical reinforcement at low strains; however, only the high structure carbon black composites did not exhibit a decrease in fracture strain at the percolation threshold; moreover the stress–strain behavior of the high structure carbon black composites conformed to the Guth hydrodynamic model.
3. A decrease in resistivity at low strains (2–

4%) and reversibility in resistivity upon cyclic loading to 20% strain differentiated composites of high structure carbon black with the ethylene–octene elastomer matrix from other low resistivity filled elastomers including vulcanized rubber composites.

4. The microstructural model proposed for the high structure carbon black composites is based on unique features of both filler and matrix, and incorporates multifunctional physical crosslinks of the ethylene–octene matrix and dynamic filler-matrix bonds.

Numerous stimulating discussions with Dr. E. V. Stepanov, CWRU, are gratefully acknowledged. The authors thank J. Chaton and C. Herd of the Columbian Chemicals Company for furnishing the carbon black and for technical support. This work was generously supported by the Army Research Office (Grant DAAG55-98-1-0311) and the National Science Foundation (Grant INT-9726537).

REFERENCES

1. Kraus, G., Ed. Reinforcement of Elastomers; Interscience: New York, 1965.
2. Boonstra, B. In Rubber Technology, 2nd ed.; Morton, M., Ed.; Van Nostrand: London, 1970; p 51.
3. Sau, K. P.; Chaki, T. K.; Khastgir, D. Polymer 1998, 39, 6461.
4. Bhattacharya, S. K., Ed. Metal-Filled Polymers; Dekker: New York, 1986.
5. Bensason, S.; Minick, J.; Moet, A.; Chum, S.; Hiltner, A.; Baer, E. J Polym Sci B Polym Phys 1996, 34, 1301.
6. Bensason, S.; Nazarenko, S.; Chum, S.; Hiltner, A.; Baer, E. Polymer 1997, 38, 3513.
7. Bensason, S.; Nazarenko, S.; Chum, S.; Hiltner, A.; Baer, E. Polymer 1997, 38, 3913.
8. Bensason, S.; Stepanov, E. V.; Chum, S.; Hiltner, A.; Baer, E. Macromolecules 1997, 30, 2436.
9. Huang, J.-C.; Huang, H.-L. J Polym Eng 1997, 17, 213.
10. Flandin, L.; Prasse, T.; Schueler, R.; Schulte, K.; Bauhofer, W.; Cavaillé, J.-Y. Phys Rev B 1999, 59, 14349.
11. Carmona, F.; Barreau, F.; Delheas, P.; Canet R. J Phys Lett 1980, 41, 531.
12. Miyasaka, K.; Watanabe, K.; Jojima, E.; Aida, H.; Sumita, M.; Ishikawa K. J Mat Sci 1982, 17, 1610.
13. Narkis, M.; Ram, A.; Stein, Z. Polym Eng Sci 1981, 21, 1049.
14. Yi, X.-S.; Wu, G.; Ma, D. J Appl Polym Sci 1998, 67, 131.
15. Flandin L.; Cavaillé J.-Y.; Bréchet Y.; Dendievel R. J Mater Sci 1999, 34, 1753.
16. Kost, J.; Foux, A.; Narkis, M. Polym Eng Sci 1994, 34, 1628.
17. Lux, F. J Mater Sci 1993, 28, 285.
18. Kirkpatrick, S. Rev Mod Phys 1973, 45, 574.
19. Zallen, R. The Physics of Amorphous Solids; Wiley: New York, 1983.
20. Derrida, B.; Stauffer, D.; Herrmann, H. J.; Vannimenus, J. J Phys Lett 1983, 44, 701.
21. Heaney, M. B. Phys Rev B 1995, 52, 12477.
22. Ibarra, L.; Macias, A.; Palma, E. Kaut Gummi Kunst 1997, 50, 478.
23. Pramanik, P. K.; Khastagir, D.; Saha, T. N. J Mater Sci 1993, 28, 3539.
24. Kurian, T.; De, P. P.; Khastgir, D.; Tripathy, D. K.; De, S. K.; Peiffer, D. G. Polymer 1995, 36, 3875.
25. Sau, K. P.; Chaki, T. K.; Khastgir, D. J Appl Polym Sci 1999, 71, 887.
26. Guth, E. J Appl Polym Sci 1945, 16, 20.
27. Huang, J.-H.; Huang, H.-L. J Polym Eng 1997, 17, 213.
28. Shui, X.; Chung, D. D. L. Smart Mater Struct 1997, 6, 102.
29. Norman, R. H. Conductive Rubbers and Plastics; Elsevier: Amsterdam, 1970.
30. Kost, J.; Narkis, M.; Foux, A. J Appl Polym Sci 1984, 29, 1984.
31. Flandin, L.; Hiltner, A.; Baer, E. Polymer, submitted.